Biomaterials 33 (2012) 7972–7983

Contents lists available at SciVerse ScienceDirect

Biomaterials

journal homepage: www.elsevier.com/locate/biomaterials

Injectable citrate-based mussel-inspired tissue bioadhesives with high wet strength for sutureless wound closure

Mohammadreza Mehdizadeh [a], Hong Weng [b], Dipendra Gyawali [b], Liping Tang [b], Jian Yang [b,c,*]

[a] Department of Materials Science and Engineering, The University of Texas at Arlington, Arlington, TX 76010, USA
[b] Department of Bioengineering, The University of Texas at Arlington, Arlington, TX 76010, USA
[c] Department of Bioengineering, The Pennsylvania State University, W340 Millennium Science Complex, University Park, PA 16802, USA

ARTICLE INFO

Article history:
Received 24 June 2012
Accepted 26 July 2012
Available online 16 August 2012

Keywords:
Bioadhesives
Hydrogels
Hemostasis
Tissue adhesion
Wound healing

ABSTRACT

The existing surgical adhesives are not ideal for wet tissue adhesion required in many surgeries such as those for internal organs. Developing surgical adhesives with strong wet tissue adhesion, controlled degradability and mechanical properties, and excellent biocompatibility has been a significant challenge. Herein, learning from nature, we report a one-step synthesis of a family of injectable citrate-based mussel-inspired bioadhesives (iCMBAs) for surgical use. Within the formulations investigated, iCMBAs showed 2.5–8.0 folds stronger wet tissue adhesion strength over the clinically used fibrin glue, demonstrated controlled degradability and tissue-like elastomeric mechanical properties, and exhibited excellent cyto/tissue-compatibility both in vitro and in vivo. iCMBAs were able to stop bleeding instantly and sutureless, and close wounds (2 cm long × 0.5 cm deep) created on the back of Sprague–Dawley rats, which is impossible when using existing gold standard, fibrin glue, due to its weak wet tissue adhesion strength. Equally important, the new bioadhesives facilitate wound healing, and are completely degraded and absorbed without eliciting significant inflammatory response. Our results support that iCMBA technology is highly translational and could have broad impact on surgeries where surgical tissue adhesives, sealants, and hemostatic agents are used.

1. Introduction

In the past two decades, clinical surgical practices have significantly benefited from using bioadhesives, tissue sealants, and hemostatic agents to control blood loss and promote tissue healing [1]. For example, biologically-derived fibrin glues, which mimic the last stage of physiological coagulation cascade, and synthetic cyanoacrylate adhesives are two well-known tissue adhesives that have been widely utilized in many applications [2–4]. Despite having advantages, such as fast curing and biodegradability, fibrin glue has relatively poor adhesion and tensile strength and its utilization involves risks of blood-borne disease transmission and potential allergic reactions to patients [4–10]. Cyanoacrylate adhesives offer advantageous properties, such as strong adhesion, rapid setting time, instantaneous adhesion to tissue, and ease of use [11]. However, concerns about complications that might occur due to the slow degradation of cyanoacrylates, the exothermic polymerization reaction, and the toxicity of degradation products, have limited the applications of cyanoacrylates mainly to topical uses [4,12]. Furthermore, both fibrin glue and cyanoacrylates work best when applied to a dry surgical field, which greatly restricts their applications for wet tissue adhesion and hemostasis required in many internal organ surgeries [13]. Currently no commercially available tissue adhesives and sealants can be broadly applied for both external and internal tissue adhesion and hemostatic applications.

Inspired by the adhesion strategy employed by some maritime creatures, such as blue mussel *Mytilus edulis* [14,15], researchers developed a new family of adhesives, which can adhere to non-specific surfaces in aqueous condition. The strong adhesion ability of the mussels has been ascribed to the presence of a catechol-containing amino acid called L-3,4-dihydroxyphenylalanine (L-DOPA), a post-translational hydroxylation of tyrosine, found in the structure of secreted mussels adhesive foot proteins [14,16,17]. Under oxidizing or alkaline condition, DOPA is believed to promote the crosslinking reactions of these adhesive proteins through the oxidation of catechol hydroxyl groups to ortho-quinone, which subsequently triggers intermolecular crosslinking, rendering cohesion and bulk elastic properties to the network of proteins. Recent studies revealed that oxidized DOPA also contributes to

* Corresponding author. Department of Bioengineering, The Pennsylvania State University, W340 Millennium Science Complex, University Park, PA 16802, USA.
E-mail address: jxy30@psu.edu (J. Yang).

0142-9612/$ – see front matter © 2012 Elsevier Ltd. All rights reserved.
http://dx.doi.org/10.1016/j.biomaterials.2012.07.055

strong adhesion to biological surfaces, through the formation of covalent bonds with available nucleophile groups on these surfaces such as $-NH_2$, $-SH$, $-OH$ and $-COOH$ groups [16,18–22]. By incorporating catechol-containing species into the structure of polymers, wet tissue adhesive hydrogel materials have been synthesized [23–28]. However, the syntheses of these catecholic polymers require costly multi-step preparation/purification techniques and the use of toxic reagents. In spite of the appealing wet tissue adhesion properties, existing mussel-inspired adhesive polymers [29,30] are essentially non-degradable thus substantially limiting their potential uses in a variety of medical applications, including tissue engineering and drug delivery. Inspired by another natural adhesion mechanism – gecko adhesion which is mainly effective on dry surfaces, biodegradable elastomer, poly(glycerol sebacate acrylate) (PGSA) was fabricated into adhesive tape with nano-pillar structures to simulate the nano-scale setae on gecko food pads [31]. To improve wet tissue adhesion, a strategy has been developed recently to coat wet tissue adhesives such as mussel-inspired adhesives [32] and aldehyde-functionalized starch [31] on gecko-adhesive structures to achieve mechanical interlocking and covalent chemistry simultaneously. Despite these exciting progresses, none of the existing bioinspired adhesives alone possess sufficient wet tissue adhesion strength and controlled degradability for sutureless wound closure application.

In the present work, we synthesized a new family of injectable citrate-based mussel-inspired bioadhesives, iCMBAs (Fig. 1). The rationale behind the iCMBA strategy was to react citric acid, poly(ethylene glycol) (PEG), and catechol-containing monomers such as dopamine or L-DOPA via a one-step polycondensation reaction. Such an approach allows us to fabricate new adhesive materials with great wet adhesion strength, controllable degradability, improved biocompatibility, and substantially reduced manufacturing costs. Citric acid, a non-toxic metabolic product of the body (Krebs cycle), was a key in our established methodology in the development of citrate-based biodegradable polymers (CBBPs) including poly(diol citrates) [33–36], crosslinked urethane-doped polyesters (CUPE) [37,38], poly(alkylene maleate citrates) (PAMC) [39–41], and biodegradable photoluminescent polymers (BPLP) [42,43] for applications in tissue engineering, drug delivery, medical devices, and bioimaging. Citric acid was mainly used to facilitate degradable ester-bond formation in biomaterials, while enhancing hemocompatibility and hydrophilicity of the polymers and providing pendant binding sites for bioconjugation to confer additional functionality such as optical properties. For iCMBA synthesis, citric acid was used to not only form degradable polyesters with PEG, but also provide valuable pendant reactive carboxyl groups to conjugate dopamine or L-DOPA. Thus, using highly reactive multifunctional citric acid enables a one-step synthesis to prepare biodegradable polyesters with pendant catechol functionalities via a facile condensation reaction. All the monomers used for iCMBA syntheses are inexpensive, readily available, and safe for in vivo uses and have been documented in many FDA (US Food and Drug administration)-approved devices and applications.

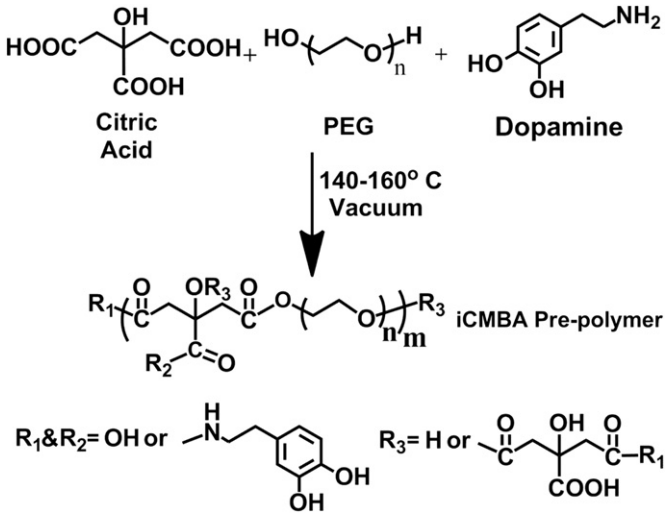

Fig. 1. Schematic representation of iCMBA pre-polymers synthesis through polycondensation reaction.

2. Materials and methods

2.1. Materials

All chemicals, cell culture medium, and supplements were purchased from Sigma Aldrich (St. Louis, MO), except where mentioned otherwise. All chemicals were used as received.

2.2. Synthesis and characterization of iCMBAs

iCMBAs are oligomers based on citric acid (CA) and PEG that have been functionalized by catechol-containing compounds, such as dopamine and L-DOPA (L-3,4-dihydroxyphenylalanine) as illustrated in Fig. 1. CA and PEG were placed in a 250 mL three-necked round-bottom flask and heated to 160 °C until a molten clear mixture was formed under stirring. Next, under nitrogen gas flow, a calculated amount of dopamine or L-DOPA was added to the mixture. After allowing enough time for a clear solution to form, the temperature was reduced to 140 °C and the reaction was continued under vacuum for the required time until the desired molecular weight was achieved. The prepared pre-polymer was dissolved in deionized (DI) water and purified by extensive dialysis using a 500 and 1000-MWCO dialysis tube. The dialyzed solution was then lyophilized to obtain the purified adhesive pre-polymer. By using different PEG lengths and various amounts of dopamine different pre-polymers of iCMBAs were synthesized as shown in Table 1.

2.3. iCMBA pre-polymers characterization

In order to characterize the functional groups present in the pre-polymers, iCMBAs were analyzed by Fourier Transform Infra Red (FT-IR) spectroscopy. 1% (w/v) solution of pre-polymers in 1,4-dioxane were cast on potassium bromide crystal discs and allowed to completely dry in a hood. The spectroscopy was then performed using a Nicolet 6700 FT-IR (Thermo Scientific, Waltham, MA) equipped with OMNIC software.

For proton analysis, 1% (w/v) solution of iCMBA pre-polymer in deuterium oxide was placed into a 5-mm-outside diameter tube and analyzed by Proton Nuclear Magnetic Resonance spectroscopy (^{1}H NMR) using a 250 MHz JNM ECS 300 (JEOL, Tokyo, Japan).

Furthermore, the presence of unoxidzied –OH groups of catechol in the structure of iCMBA pre-polymers was determined by UV–VIS spectroscopy [44], where absorbance of 0.02% (w/v) solution of various pre-polymers in DI water were measured using Shimadzu UV–VIS spectrophotometer machine across the wavelength of 700–200 nm.

2.4. Crosslinking of iCMBAs and gel time measurement

In order to crosslink the iCMBAs and make adhesive hydrogels, pre-polymers were first dissolved in Phosphate Buffer Saline (PBS) solution and then mixed with sodium (meta) periodate (PI) solution in DI water. PI is an oxidizing agent, which triggers oxidation and consequently crosslinking reaction of catechol-containing iCMBAs upon mixing.

Gel or set time was determined by a viscometry technique based on modified ASTM D4473 method using a cone and plate Brookfield viscometer (Brookfield Engineering Labs, Inc, MA) equipped with temperature control unit. For this purpose 1 mL of 50% (w/w) solution of pre-polymer in PBS was mixed with equal volume of PI solution with different concentrations to achieve various PI/pre-polymer ratios. Immediately after mixing the mixture was transferred to the viscometer cup and the viscosity of the mixture was measured versus time, using a CP-42 spindle at spinning speed of 12 revolutions per minutes. The time from the start point till onset of abrupt increase in the viscosity of the mixture, determined according to ASTM D4473, was defined as the gel time of polymer adhesives. The measurements were done at 25 °C for all samples except for iCMBA-$P_{400}D_{0.5}$ PI:8%, which was measured at two temperatures, 25 °C and 37 °C, to evaluate the influence of temperature on the gel time. Different iCMBA formulations and various ratios of PI to iCMBA pre-polymers were tested to study the influence of PEG molecular weight, the amount

Table 1
Nomenclature, feeding ratio, and final composition ratio of pre-polymers.

Polymer name	Molecular weight of used PEG (Da)	CA:PEG:dopamine (moles)	CA:PEG:dopamine feeding ratio	CA:PEG:dopmaine composition ratio
iCMBA-$P_{400}D_{0.1}$	400	1.1:1:0.1	0.50:0.45:0.05	0.49:0.46:0.05
iCMBA-$P_{400}D_{0.3}$	400	1.1:1:0.3	0.46:0.42:0.12	0.46:0.43:0.11
iCMBA-$P_{400}D_{0.5}$	400	1.1:1:0.5	0.42:0.38:0.20	0.41:0.42:0.17
iCMBA-$P_{200}D_{0.3}$	200	1.1:1:0.3	0.46:0.42:0.12	0.46:0.44:0.10
iCMBA-$P_{1000}D_{0.3}$	1000	1.1:1:0.3	0.46:0.42:0.12	0.45:0.46:0.09

of dopamine in the structure of pre-polymer, and the effect of initiator-to-prepolymer ratio on the crosslinking, gel time and properties of iCMBAs.

2.5. Properties of crosslinked iCMBAs

Mechanical properties of crosslinked polymers, including ultimate tensile strength, modulus and elongation at break, were measured according to ASTM D412A on a MTS Insight 2 fitted with a 10 N load cell (MTS, Eden Prairie, MN). Briefly, the dog bone shaped samples (25 mm × 6 mm × 1.5 mm, length × width × thickness) were pulled at a rate of 500 mm/min, and elongated to failure. Values were converted to stress–strain and the initial modulus was calculated from the initial slope of the curve (0–10% elongation). In order to evaluate the effect of hydration on the mechanical properties of crosslinked iCMBAs, the mechanical tests were also conducted on the fully swollen samples, i.e. samples that have been hydrated and swollen in water for 4 h.

For sol content measurement polymer cylindrical discs (5 mm diameter; 2 mm thick) were cut from unpurified crosslinked films. The discs were weighed to find the initial mass (W_i), and suspended in 1,4-dioxane for 48 h while the solvent was changed every 6 h. Next, the samples were removed from the solvent and lyophilized for 72 h. The dried samples, absent of any unreacted prepolymers, were weighed to find the dry mass (W_d). The sol–gel fraction was calculated using the formula from equation (1):

$$\text{Sol}\ (\%) = \frac{W_i - W_d}{W_i} \times 100 \quad (1)$$

To measure swelling ratio the leached and dried samples were then suspended in water for 24 h. Next, samples were removed from the water, blotted dry with filter paper, and weighed (W_s). The swelling percentage was calculated using the formula from equation (2):

$$\text{Swelling}\ (\%) = \frac{W_s - W_d}{W_d} \times 100 \quad (2)$$

Degradation studies were conducted in PBS (pH 7.4). Cylindrical disc specimens (7 mm in diameter; 2 mm thick) were cut from purified crosslinked films. The samples were weighed (W_0), placed in test tubes containing 10 mL of PBS and incubated at 37 °C for pre-determined time points and till complete degradation of polymer. PBS was changed every 12 h. After incubation for pre-determined time points, samples were thoroughly washed with deionized water, lyophilized for 72 h, and weighed. The mass loss was calculated by comparing the initial mass (W_0) with the mass measured at the pre-determined time points (W_t), as shown in equation (3).

$$\text{Mass loss}(\%) = \frac{W_0 - W_t}{W_0} \times 100 \quad (3)$$

2.6. Adhesion strength measurement

The adhesion strengths of different formulations were determined by lap shear strength test according to modified ASTM D1002-05 method. Briefly, strips of porcine-derived, acellular small intestine submucosa (SIS) material (OASIS®, HealthPoint Ltd. Fort Worth, TX) were prepared in 40 × 4 mm dimension. After mixing the iCMBA solution with determined amount of PI solution, 10 μL of the mixture was dispensed and spread over an area of 6 × 4 mm of one strip, which was pre-soaked in water. A second wet strip was subsequently brought in contact with the first one to form a contact area of 6 × 4 mm. The adhered strips were then placed in a highly humid chamber for 2 h. The lap shear strength of bonded strips specimens were subsequently measured using MTS Insight 2 fitted with a 10 N load cell and crosshead speed of 1.3 mm/min (MTS, Eden Prairie, MN). Besides various formulations of iCMBAs, fibrin glue (Tisseel, Baxter healthcare Corp.) was also tested as a control.

2.7. In vitro biocompatibility tests of iCMBAs

To quantitatively assess in vitro pre-polymer cytotoxicity a methlythiazoletetrazolium (MTT) cell proliferation and viability assay was performed. First, the solution of different iCMBAs pre-polymers in Dulbecco's modified eagle's medium (DMEM), containing 10% (v/v) fetal bovine serum (FBS) and 1% (v/v) streptomycin, were prepared in 3 different concentrations: 10, 1 and 0.1 mg/mL (pre-polymer/medium). Next, to each well of a 96-well cell culture plate, 200 μL of solution of NIH 3T3 fibroblast cells in DMEM, with concentration of 5×10^4 cells/mL, was added and incubated for 24 h at 37 °C, 5% CO_2 and 95% relative humidity. The medium of each well was then replaced by pre-polymer-containing DMEM solutions with various concentrations and incubated for another 24 h followed by MTT assay analysis as per the manufacturer's protocol. Poly(ethylene glycol) diacrylate (PEGDA, $M_n = 700$) solutions were used as control as previously described [39]. Viability of cells in the DMEM containing pre-polymers and PEGDA were normalized to that of cells cultured in blank medium (DMEM without pre-polymers) as control.

Cytotoxicity of sol content or leachable fraction of crosslinked iCMBAs, referred to as sol-cytotoxicity, was also assessed by incubating equal mass of crosslinked iCMBA samples in 5 mL cell culture medium for 24 h. Next, three different solutions were prepared: 1×, 10× and 100× (1× was the solution of leached products with no dilution; 10× and 100× means 10 times and 100 times dilution of 1× by medium, respectively) which were used for cell culture. Fibrin glue (Tisseel, Baxter Corp.) and blank medium were used as controls. To evaluate the degradation products cytotoxicity, various formulations of crosslinked iCMBAs films (equal weight of each polymer) were fully degraded in 10 mL complete cell culture medium. The resultant solutions were diluted to three concentrations (1×, 10× and 100×) using DMEM, and used for cell culture and subsequent MTT analysis. All the above solutions were pH-neutralized and passed through a 0.2 μm filter prior to use for cell culture. Qualitative cytotoxicity evaluation was also carried out by observing the adhesion of NIH 3T3 fibroblast cells to crosslinked iCMBAs films under light microscope. Briefly, crosslinked iCMBA films were cut in discs (5 mm diameter and 1 mm thickness) and sterilized by incubation in 70% ethanol for 3 h followed by exposure to UV light for 3 h. 200 μL of 3T3 fibroblast cell solution (5×10^4 cells/mL) was then seeded on the films. Using a photomicroscope, Nikon Eclipse Ti-U equipped with DS-Fi1 camera (Nikon Instruments Inc, Melville NY) the morphology of cells on the films were observed and pictured at day-1,3, and 5 post seeding.

2.8. In vivo study

The in vivo biocompatibility and wound healing properties of the iCMBAs were tested using rat skin incision model [45]. All experiments were performed with the approval of the University of Texas at Arlington Animal Care and Use Committee (IACUC). Sprague–Dawley rats (female, average weight of 300 ± 50 g, 5 animals/group) were sedated with intraperitoneal injection of ketamine (40 mg/kg) and xylazine (5 mg/kg). Skin surgical area was sterilized with betadine and followed by 70% ethanol. Six full-thickness wounds (2 cm long × 0.5 cm deep) were made on the dorsum of each rat. Three of the wounds on each rat were closed by dropping sterilized iCMBA-$P_{400}D_{0.5}$ PI:8% into the wounds followed by finger-clamping for about 2 min while three other wounds were closed by conventional suturing as control. To minimize variations in surgical intervention, one surgeon performed all the procedures in a uniform fashion. On the 7th and 28th day post-wounding, the test animals were sacrificed and skin tissue at wound sites were excised for histological analyses. These sections were stained with hematoxylin and eosin (H&E) for morphological assessment and Masson trichrome staining was used to assess the collagen production. To evaluate inflammatory cells, immunohistochemistry was performed to quantify the number of CD11b positive cells. The tissue sections were stained with inflammatory cell marker CD11b (rabbit anti-rat Integrin αM, H-61, Santa Cruz Biotechnology), and peroxidase-conjugated goat anti-rabbit secondary antibodies (Santa Cruz Biotechnology). All histological imaging analyses were performed on a Leica microscope (Leica, Wetzlar, Germany). Cell infiltration into the incision area was quantified using Image J software [46] by calculating cell density (number of cells per unit area) in random areas in the proximity of incision line with area held constant for all samples. The number of CD11b positive cells in the incision area was also determined by counting the cells in the cell infiltration area. Collagen density (as %) was determined through Masson trichrome staining images by calculating the ratio of blue-stained area to total area using Image J. The healing and reconstruction of tissue in the incision area after four weeks was also evaluated by measuring the tensile mechanical strength of the regenerated tissue treated with iCMBA and comparing it with suture-closed wounds [45].

2.9. Statistical analysis

All data were presented as means ± standard deviations, with sample number of at least 5. The significance of differences between results was evaluated by One-Way

ANOVA test. In some tests, the value of $p < 0.05$ (*) and in some others $p < 0.01$(**) were considered to be statistically significant.

3. Results

3.1. Synthesis and characterization of iCMBA pre-polymers

iCMBA pre-polymers were synthesized in a convenient one-step polycondensation reaction between citric acid, PEG, and dopamine without requiring any organic solvent or toxic reagent. The FTIR spectra of some iCMBA pre-polymers as well as the spectrum of poly (citrate-PEG) are shown in Fig. 2A. The peak at 1527 cm^{-1} were assigned to amide group (C(=O)–NH) which is not observed in CA-PEG. Peaks between 1700 and 1750 cm^{-1} were assigned to carbonyl group (C=O) in amide and ester bonds. The relatively broad peaks centered at 2931 cm^{-1} were assigned to methylene groups which were observed in all the spectra of the iCMBA pre-polymers. The broad peaks centered at 3435 cm^{-1} were assigned to the hydroxyl group stretching vibration and hydrogen bonded unreacted-carboxyl groups [47].

A representative spectrum of ^{1}H NMR analysis of purified iCMBA pre-polymer is depicted in Fig. 2B. The chemical shifts at 6.4–6.7 ppm were assigned to protons of phenyl group which is a characteristic of catechol group present in the structure of iCMBAs [48]. The multiple peaks between 2.55 and 2.90 ppm were assigned to the protons in methylene groups from citric acid and dopamine [49]. The large peak at 3.45 ppm was attributed to the protons signal of $-OCH_2-CH_2-$ from PEG and the shifts detected at 4.1–4.2 ppm were from methylene groups of PEG adjacent to ester bond. The composition ratios of the iCMBA pre-polymers, shown in Table 1, were calculated by comparing the area under peaks of phenyl protons shifts with that of assigned to protons of citric acid and PEG methylene groups.

The results of UV–VIS photospectroscopy showed the absorption of UV light at 280 nm wavelength for all samples, as displayed in Fig. 2C. iCMBA-$P_{400}D_{0.5}$ and iCMBA-$P_{200}D_{0.3}$ showed the highest absorption of UV at 280 nm followed by iCMBA-$P_{400}D_{0.3}$, iCMBA-$P_{1000}D_{0.3}$ and iCMBA-$P_{400}D_{0.1}$.

3.2. Crosslinking and gel time of iCMBAs

The gel times of different compositions are shown in Table 2, which have been derived from viscosity measurements (Fig. 2D) of

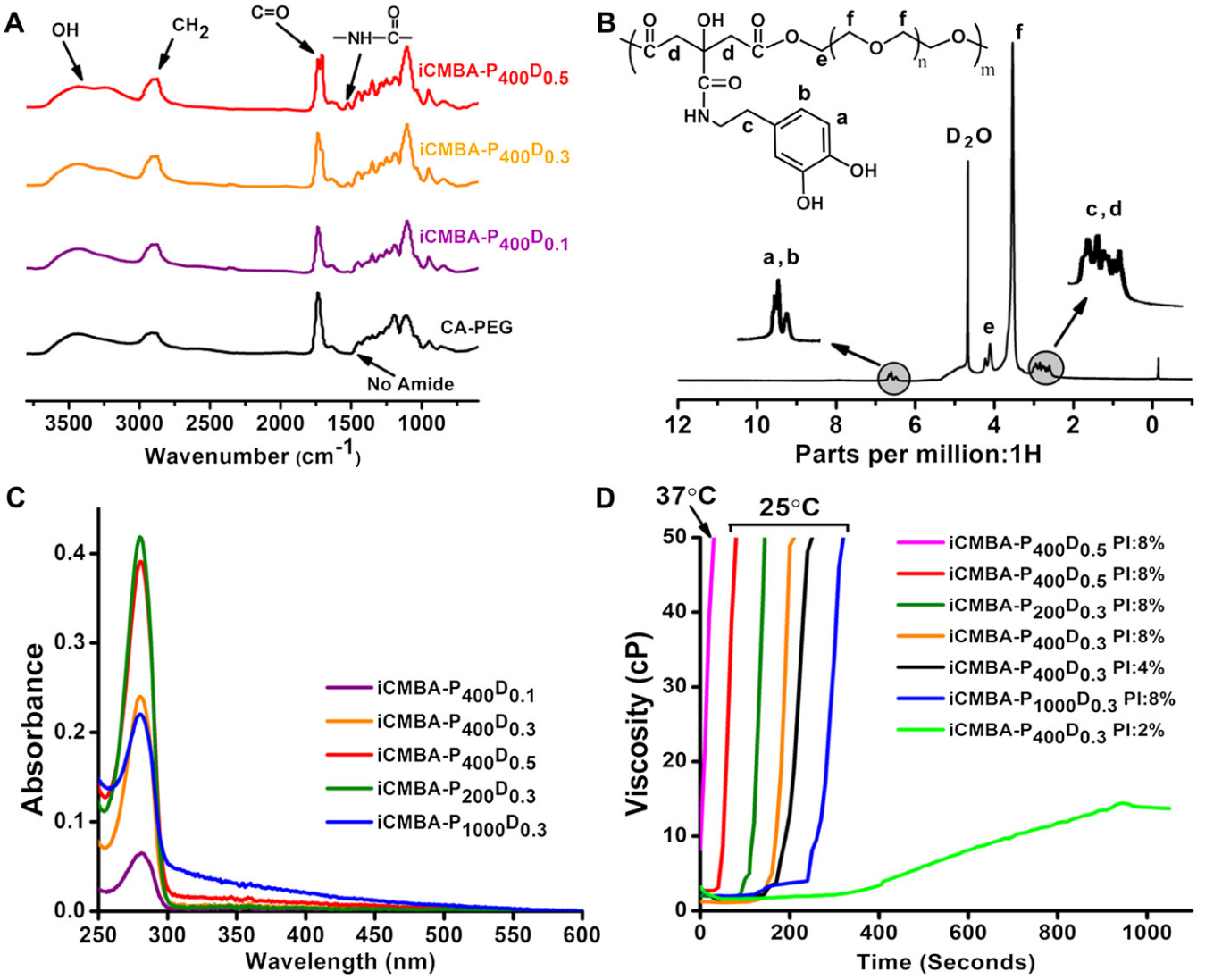

Fig. 2. Characterization and gel time measurement of iCMBAs. A) FTIR spectra of different iCMBAs. B) ^{1}H NMR spectrum of a representative iCMBA. C) UV–VIS absorption spectra of iCMBAs, measured on 0.02% pre-polymer solutions in deionized water. D) Viscosity changes versus time for different iCMBAs being crosslinked with various ratios of sodium periodate (PI).

Table 2
Gel time of different iCMBAs crosslinked by various ratios of sodium periodate (PI) to polymer (measured by viscometry).

Polymer name	PI to pre-polymer ratio (w/w%)	Test temperature (°C)	Measured gel time (s)
iCMBA-$P_{400}D_{0.5}$	8%	37	18 ± 2
iCMBA-$P_{400}D_{0.5}$	8%	25	46 ± 4
iCMBA-$P_{200}D_{0.3}$	8%	25	97 ± 3
iCMBA-$P_{400}D_{0.3}$	8%	25	163 ± 9
iCMBA-$P_{400}D_{0.3}$	4%	25	175 ± 13
iCMBA-$P_{1000}D_{0.3}$	8%	25	244 ± 11
iCMBA-$P_{400}D_{0.3}$	2%	25	313 ± 10

iCMBAs during crosslinking reaction after mixing with initiator. The measured gel times were in the range of 18 s for iCMBA-$P_{400}D_{0.5}$ PI:8% at 37 °C up to slightly over 5 min for iCMBA-$P_{400}D_{0.3}$ PI:2%. Higher amount of dopamine in the structure of pre-polymer decreased the gel time as did higher initiator-to-prepolymer ratio. iCMBA pre-polymers made with higher molecular weight PEG exhibited longer gel time, when crosslinked with the same amount of PI.

3.3. Properties of crosslinked iCMBAs

Mechanical properties of crosslinked iCMBAs in dry and fully hydrated states are tabulated in Table 3. In the dry state, the highest measured values for tensile strength, elongation at break and tensile modulus were 8515.1 ± 1167 kPa (iCMBA-$P_{200}D_{0.3}$ PI:8%), 1582.5 ± 144.6% (iCMBA-$P_{400}D_{0.3}$ PI:4%) and 35.7 ± 6.7 MPa (iCMBA-$P_{200}D_{0.3}$ PI:8%), respectively. The stress–strain curves of crosslinked iCMBAs are also shown in Fig. 3A. All iCMBAs demonstrated a rubber-like (elastomer) behavior. As shown in Table 3, the mechanical properties decreased when samples were hydrated and swollen, which is expected for hydrophilic iCMBAs.

The degradation studies of the polymers revealed that the disintegration rate was inversely related to the degree of crosslinking, as expected. As shown in Fig. 3B, iCMBA-$P_{400}D_{0.5}$ PI:8% exhibited the slowest rate of degradation, 25 days for complete degradation in PBS at 37 °C. For the same reason, iCMBA-$P_{400}D_{0.1}$ was rapidly disintegrated within less than one day. On the other hand, using PEG with higher molecular weight accelerated the degradation of polymers as can be observed from faster degradation of iCMBA-$P_{1000}D_{0.3}$ (PEG 1000) compared to iCMBA-$P_{400}D_{0.3}$ (PEG 400) and iCMBA-$P_{200}D_{0.3}$ (PEG 200) with an identical PI-to-prepolymer ratio (8%).

Sol contents of different crosslinked iCMBAs are shown in Fig. 3C. iCMBA-$P_{400}D_{0.5}$ and iCMBA-$P_{200}D_{0.3}$, both crosslinked with PI:8% (w/w PI/pre-polymer), showed the lowest amount of sol content of 2.37% and 2.86%, respectively. iCMBA-$P_{400}D_{0.3}$ PI:2% had the highest sol content of about 34%. The evaluation of swelling ratios of crosslinked polymers showed that iCMBA-$P_{400}D_{0.5}$ PI:8%, having the highest amount of dopamine content and crosslinked with high PI-to-iCMBA ratio, demonstrated the lowest swelling percentage with 471.8% as shown in Fig. 3D. On the other hand iCMBA-$P_{1000}D_{0.3}$ PI:8%, which consists of PEG 1000, displayed the highest swollen ratio at approximately 3400%.

3.4. Adhesion strength

The lap shear adhesion strength of different iCMBA formulations varied between 33.4 ± 8.9 kPa (for iCMBA-$P_{200}D_{0.3}$ PI:2%) and 123.2 ± 13.2 kPa (for iCMBA-$P_{1000}D_{0.3}$ PI:8%), which were at least two folds stronger than commercially available fibrin glue with the adhesion strength measured at 15.4 ± 2.8 kPa, as shown in Fig. 4 and Table 4.

3.5. In vitro cell viability and proliferation

The results of cytotoxicity of pre-polymers are shown in Fig. 5A. At the concentration of 10 mg/mL (pre-polymer/cell culture medium) the cell viability was between 66 ± 6 and 78 ± 11% of that in the blank medium, which was comparable to the value for control solution (PEGDA 700) at 78 ± 7%, and there were no significant differences between different pre-polymers. In diluted solutions of 1 and 0.1 mg/mL the cell viability was approximately similar to what measured for blank medium and PEGDA. The cytotoxicity of the leachable content (sol content) of crosslinked iCMBAs at 1× concentration was between of 60 ± 4 and 83 ± 14%, showing minor to moderate cytotoxicity, which was directly proportional to the sol content of each polymer and the amount of PI (8%) (Fig. 5B). Furthermore, iCMBA degradation products (1×) showed a cell viability of at least 72.9 ± 9%, suggesting that the degradation products of all crosslinked iCMBAs did not induce significant cytotoxicity (Fig. 5C). The qualitative examination of NIH 3T3 fibroblast cells by light microscopy demonstrated an excellent cell attachment to the iCMBA films and the expected morphology. The proliferation of the cells was also observable through three time points (Fig. 5D–F).

3.6. In vivo study

During animal study, upon applying iCMBAs the bleeding of created incisions on the dorsum of Sprague–Dawley rats was immediately impeded and the wound openings were closed within 2 min (Fig. 6A). Furthermore, the visual examination and comparison of iCMBA-treated and sutured wounds at different time points demonstrated the high efficiency of iCMBAs in the wound healing process (Figs. 6B, C and 7A–C). The histological evaluation (H&E staining) at day seven showed only minor acute inflammation when iCMBA was utilized. The difference between total cell densities in the incision area treated by iCMBA (7th day = 3996 ± 264 #/mm^2; 28th day = 3202 ± 227 #/mm^2) and suture (7th day: 4117 ± 269 #/mm^2; 28th day: 2992 ± 163 #/mm^2) was not significant (Fig. 6D–G, P). Similarly the number of CD11b positive inflammatory cells in the incisions area at seventh day post treatment was not significantly different in iCMBA-treated wounds (1771 ± 242 #/mm^2) and sutured wounds (1592 ± 142 #/mm^2). By

Table 3
Mechanical properties of different iCMBAs crosslinked at various prepolymer-to-sodium periodate (PI) ratios, in dry and fully hydrated (swollen) states.

Polymer name	PI to pre-polymer ratio (w/w%)	Tensile strength (kPa)		Elongation at break (%)		Modulus (MPa)	
		Dry	Swollen	Dry	Swollen	Dry	Swollen
iCMBA-$P_{400}D_{0.3}$	2	1082.6 ± 166.4		962.2 ± 78.1		0.356 ± 0.05	
iCMBA-$P_{400}D_{0.3}$	4	1644 ± 84.3		1582.5 ± 144.6		0.73 ± 0.05	
iCMBA-$P_{400}D_{0.3}$	8	2067.3 ± 732	69 ± 7	911.8 ± 405.8	143.5 ± 46	1.61 ± 0.66	0.068 ± 0.007
iCMBA-$P_{400}D_{0.5}$	8	2931.4 ± 514.9	216 ± 57.2	296.1 ± 83.9	41.6 ± 6	2.61 ± 0.57	0.69 ± 0.14
iCMBA-$P_{200}D_{0.3}$	8	8515.1 ± 1167	242.4 ± 52.3	397.4 ± 26.4	210 ± 97.2	35.7 ± 6.7	0.202 ± 0.07
iCMBA-$P_{1000}D_{0.3}$	8	3496 ± 806.2	82.8 ± 3.6	201.4 ± 49	132 ± 32.1	33.4 ± 11.9	0.091 ± 0.005

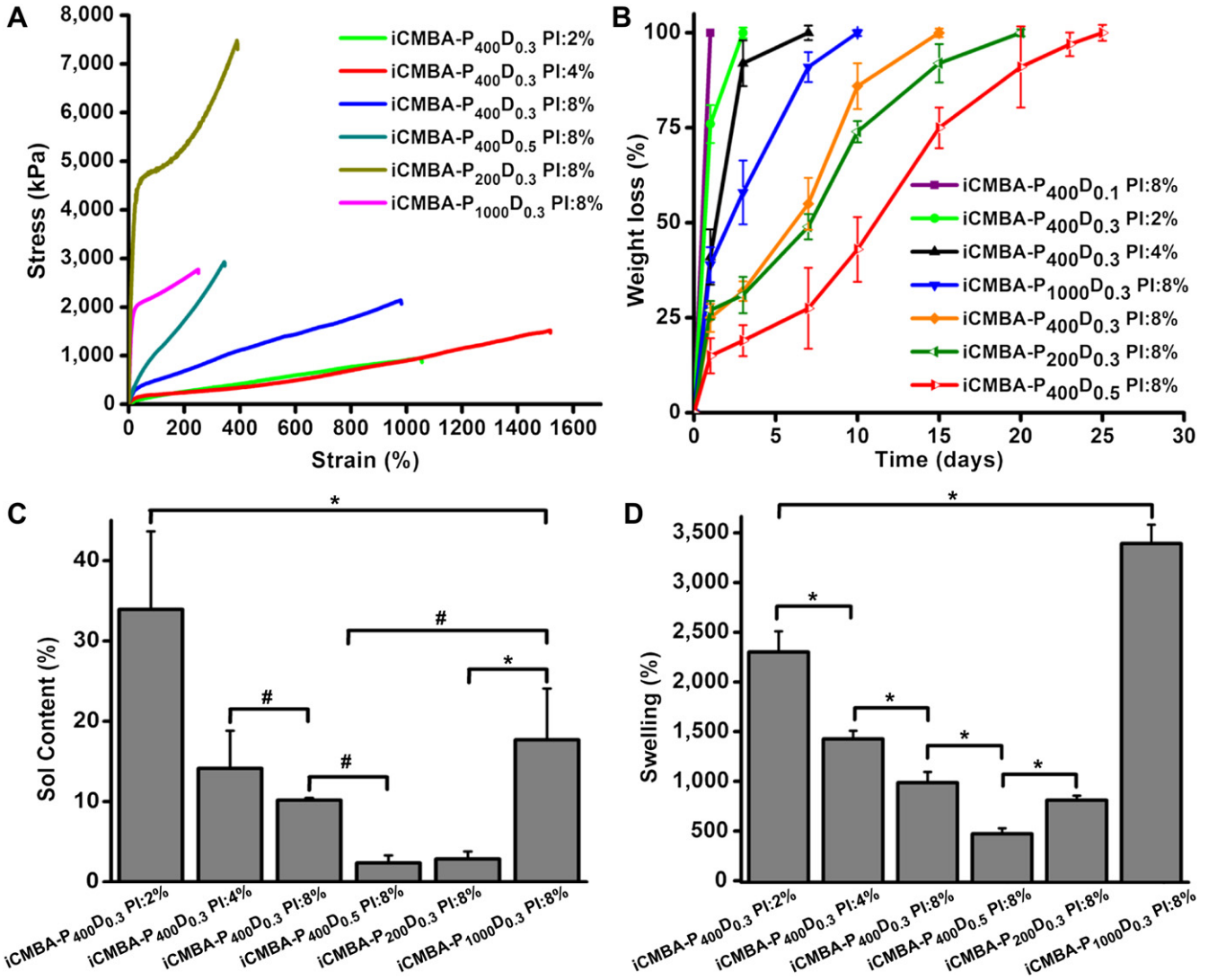

Fig. 3. Mechanical properties, degradation, sol content and swelling of crosslinked iCMBAs. A) Stress-strain curve of crosslinked iCMBAs. B) Degradation profile of crosslinked iCMBAs incubated in PBS (pH7.4) at 37 °C. C) Sol content, and D) Swelling ratios of iCMBAs crosslinked with various sodium periodate (PI) to pre-polymer ratios.

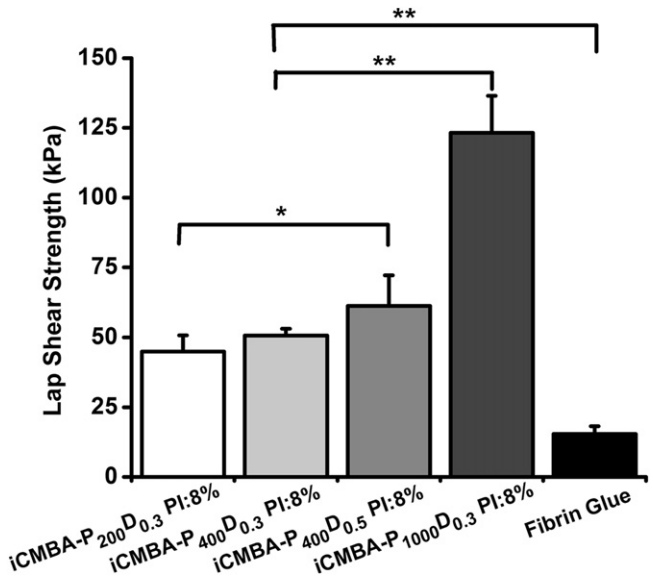

Fig. 4. Adhesion strength of iCMBAs and fibrin glue to wet porcine small intestine submucosa measured through lap shear strength test (**$p < 0.01$, *$p < 0.05$).

day 28th there was a negligible number of inflammatory cells for both groups (iCMBA: 92 ± 42 #/mm^2; suture: 107 ± 50 #/mm^2) (Fig. 6H–K, Q). In addition, a higher amount of collagen was found at the sites of rat's iCMBA-treated wounds (7th day = 15 ± 12%; 28th day = 63 ± 4%) than those treated with sutures (7th day = 17 ± 9%; 28th day = 58 ± 7%) on day 28th (Fig. 6L–O, R). The measurement of mechanical properties of rat skin revealed that the

Table 4
Wet tissue adhesion strength of different iCMBAs and fibrin glue on small intestin submucosa measured by lap shear strength test.

Polymer name	PI to pre-polymer ratio (w/w%)	Lap shear strength (kPa)
iCMBA-P$_{400}$D$_{0.3}$	2%	39.09 ± 7
iCMBA-P$_{400}$D$_{0.3}$	4%	40.4 ± 2.79
iCMBA-P$_{400}$D$_{0.3}$	8%	50.73 ± 2.43
iCMBA-P$_{400}$D$_{0.5}$	8%	61.3 ± 10.87
iCMBA-P$_{200}$D$_{0.3}$	2%	33.41 ± 8.93
iCMBA-P$_{200}$D$_{0.3}$	4%	33.84 ± 5.26
iCMBA-P$_{200}$D$_{0.3}$	8%	44.99 ± 5.76
iCMBA-P$_{1000}$D$_{0.3}$	2%	49.34 ± 6.49
iCMBA-P$_{1000}$D$_{0.3}$	4%	90.25 ± 11.25
iCMBA-P$_{1000}$D$_{0.3}$	8%	123.23 ± 13.23
Fibrin glue	-	15.38 ± 2.82

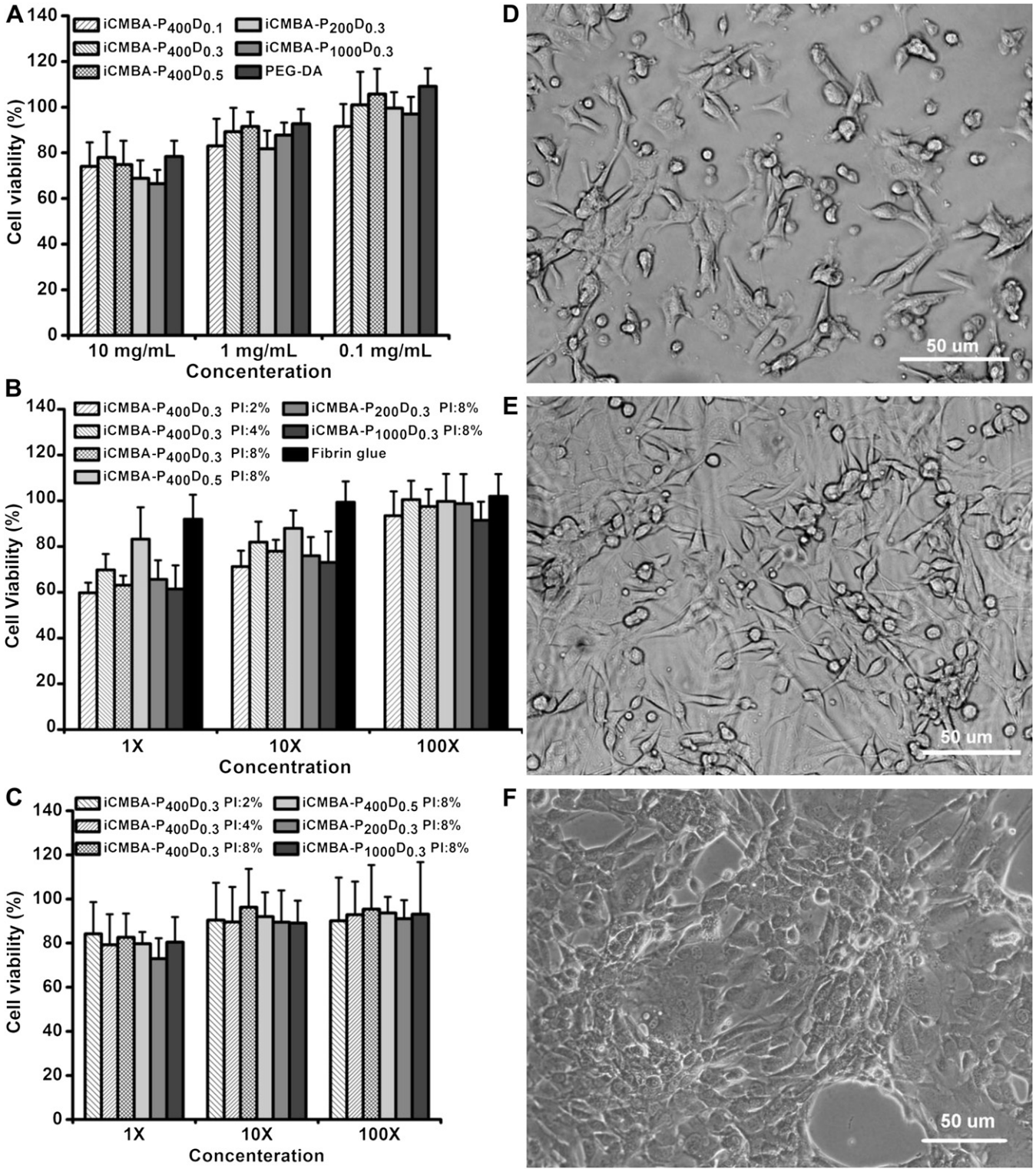

Fig. 5. In vitro cytotoxicity evaluation of iCMBAs. Cytotoxicity study using NIH 3T3 fibroblast cells by MTT assay for: A) iCMBA pre-polymers and poly(ethylene glycol) diacrylate (PEGDA) control, B) Leachable products (sol content) of crosslinked iCMBAs and fibrin glue control, and C) degradation products of crosslinked-iCMBAs. All data were normalized to cell viability in blank medium. D, E, and F) Light micrographs of NIH 3T3 fibroblast cells seeded on iCMBA films at 1st day, 3rd day, and 5th day post seeding, respectively.

iCMBA-treated skin had better tensile strength (1250 ± 315 kPa) than suture-closed skin (810 ± 355 kPa), while modulus and elongation at break were similar for both groups (Fig. 7D, E). The examination of the healed wounds after 28 days showed no trace of polymer at the location of healed tissue, suggesting that iCMBAs were fully degraded in the rat body (Fig. 7C).

4. Discussion

iCMBAs were synthesized by a single-step polycondensation reaction between citric acid, polyethylene glycol and dopamine (Fig. 1). The FTIR and ^{1}H NMR characterizations confirmed the esterification reaction between CA and PEG, and formation of amid

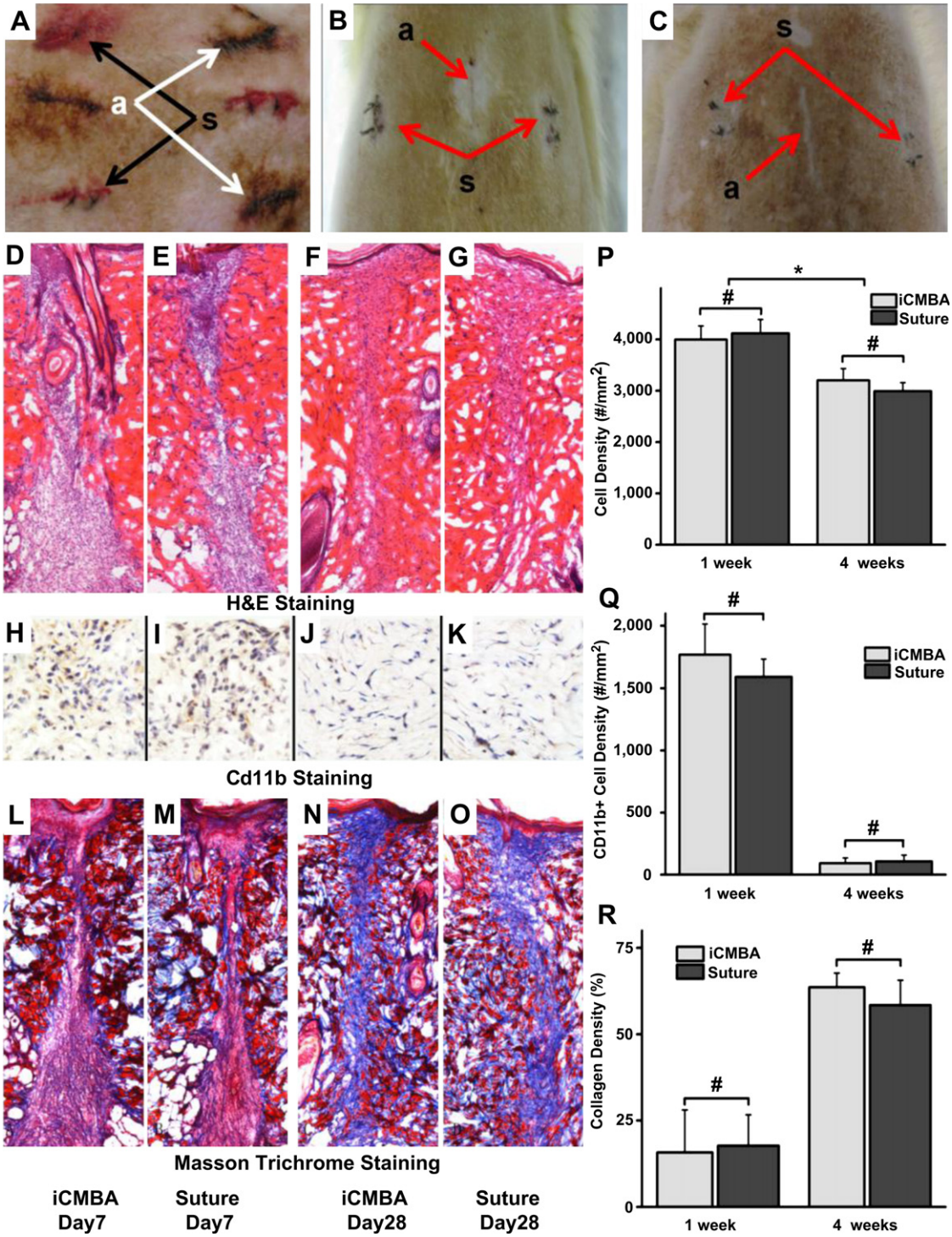

Fig. 6. Histological evaluation of rat skin closure and wound repair. Images of a rat's dorsum skin with created wounds that were closed by iCMBA (a) and suture (s): A) 2 min, B) 7 days, and C) 28 days post operation. D–O) Images of H&E (hematoxylin and eosin), immunohistochemical (for CD11b), and Masson trichrome stainings of sections of wounds at 7th day post treatment with iCMBA (D, H and L) and suture (E, I, and M); and at 28th day post treatment with iCMBA (F, J, and N) and suture (G, K, and O) (original magnification: 200× for D–G, and L–O and 400× for H–K). P) Total cell density infiltrated into the area surrounding the incision 1 week and 4 weeks post treatment with iCMBA and suture. Q) Number of CD11b positive cells in the vicinity of wounds treated with iCMBA and suture. R) Collagen density in the wound area at 1- and 4-week time points (#$p > 0.05$).

linkage between the unreacted –COOH groups of CA and dopamine's $-NH_2$ groups (Fig. 2A, B). ^{1}H NMR also revealed that the compositional ratio of iCMBA pre-polymers was consistent with the feeding ratio, a sign of high yield of this synthesis method (Table 1).

The UV–VIS photospectroscopy proved the availability of catechol hydroxyl groups in the pre-polymers structure through the observation of UV light absorption at 280 nm wavelength for all samples (Fig. 2C) [44]. The presence of unoxidized catechol groups is essential for adhesion and crosslinking processes to take place [14,16,18–22]. In the pre-polymers with high molecular weight PEG (M_n = 1000, for example) the UV absorption was weaker than expected, which can be related to the reduced amount of available unoxidized hydroxyl groups presumably due to the possible partial

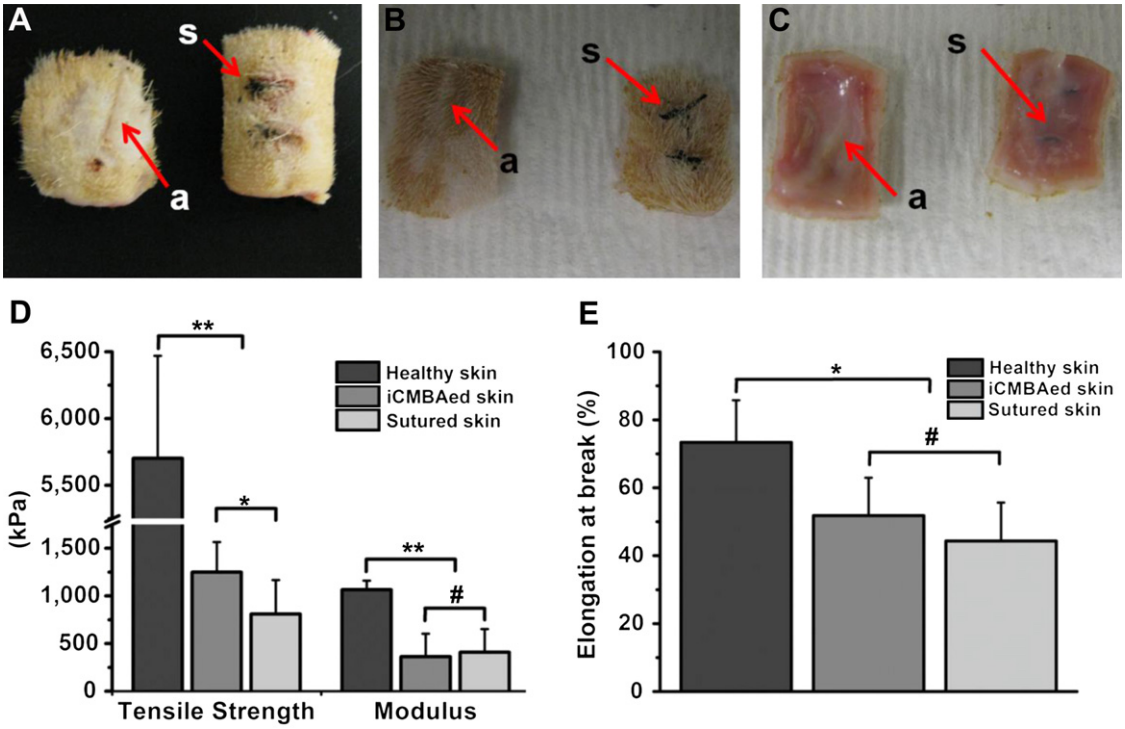

Fig. 7. Tensile tests on healed skins closed by iCMBA (a) and suture (s). The pieces of excised skin tissue of sacrificed rats at the site of wounds treated with iCMBA and suture at 7th day (A) and 28th day (B and C: reverse side) post operation. Note the enhanced healing of the wounds closed by iCMBA over sutured wounds. D) Tensile strength and Young's modulus of healthy skin and healed skin closed by iCMBA and suture at 28th days. E) Elongation at failure for the same study groups ($^{**}p < 0.01$, $^{*}p < 0.05$ and $\#p > 0.05$).

oxidation of the catechol groups over the course of longer synthesis time of these pre-polymers. This was evident from the smaller absorption peak of iCMBA-$P_{1000}D_{0.3}$ at 280 nm compared to iCMBA-$P_{400}D_{0.3}$ and iCMBA-$P_{200}D_{0.3}$. Oxidation of catechol hydroxyl groups to quinone could also be verified by UV absorption of quinone group at around 390 nm [44].

Based on proposed crosslinking mechanisms of mussel adhesive proteins [48], the plausible crosslinking and adhesion mechanisms for iCMBAs are shown in Fig. 8. The gel times ranged between 18 ± 2 and 313 ± 10 s (Fig. 2D and Table 2) and were a function of multiple factors. Increasing the oxidant (PI)-to-prepolymer ratio, incorporating more dopamine in the pre-polymer structure, and using PEG with smaller molecular weight resulted in faster gel formation. The sol content and swelling data also confirmed the crosslinking of the pre-polymers, which were in agreement with the expected degree of crosslinking (Fig. 3C, D).

The evaluation of mechanical properties of crosslinked iCMBA suggested that these materials demonstrated rubber-like behavior with typical stress-strain curves of elastomers (Fig. 3A), which is especially important for soft tissue adhesives, which must mechanically remain in harmony with flexible soft tissues for better load bearing and stress transferring. Tensile strength, elongation at break and modulus of iCMBAs varied with the molecular weight of PEG and the degree of crosslinking, which was itself a function of the amount of dopamine in the pre-polymer structure and the amount of crosslinking initiator (PI) (Table 3). Thus, the mechanical properties can be easily tuned according to requirements.

The degradation profile of the crosslinked iCMBAs revealed one of the unique features of our synthesized adhesives: the degradability of these adhesive biomaterials within a limited period of time (Fig. 3B). The degradation rate was inversely related to the level of crosslinking, as expected. iCMBA-$P_{400}D_{0.5}$ PI:8% exhibited the slowest rate of degradation, 25 days for complete degradation in PBS at 37 °C, due to higher crosslinking level. On the contrary, iCMBA-$P_{400}D_{0.1}$ PI:8%, which was inadequately crosslinked due to low catechol (dopamine) content, rapidly disintegrated within less than one day. The presence of higher-molecular-weight PEG in the polymer structure, which conferred more hydrophilicity to the polymer, accelerated the degradation of polymers, as can be observed from faster degradation of iCMBA-$P_{1000}D_{0.3}$ compared to iCMBA-$P_{400}D_{0.3}$ and iCMBA-$P_{200}D_{0.3}$, all crosslinked with the same PI-to-prepolymer ratio (8%).

Within the formulations investigated, the wet tissue bonding strength of the iCMBAs was 2.5–8.0 folds higher than that of fibrin glue ($p < 0.01$)(Fig. 4 and Table 4). Thereof, the lowest bonding strength among iCMBAs belonged to iCMBA-$P_{200}D_{0.3}$ PI:2% (33.41 ± 8.93 kPa), which was at least two folds higher than that of the gold standard, fibrin glue, measured at 15.38 ± 2.82 kPa. Adhesives based on iCMBA-$P_{1000}D_{0.3}$ demonstrated the strongest adhesion to SIS adherents, followed by iCMBA-$P_{400}D_{0.5}$. Bonding strength of iCMBA-$P_{400}D_{0.3}$ adhesive polymers was higher than iCMBA-$P_{200}D_{0.3}$ polymers ($p < 0.05$). However, there were no significant differences within iCMBA-$P_{400}D_{0.3}$ group or iCMBA-$P_{200}D_{0.3}$ group when crosslinked with different PI ratios (Table 4).

The quantitative in-vitro cytotoxicity evaluations of iCMBA prepolymers, sol (leachable), and degradation products of crosslinked iCMBAs suggested that the tested formulations did not induce significant cytotoxicity to NIH 3T3 fibroblast cells (Fig. 5A–C). These results along with qualitative cell proliferation and morphological assessment (Fig. 5D–F) supported that this family of bioadhesive polymers are suitable candidates for biological and biomedical applications.

In vivo studies confirmed the effectiveness and convenience of using iCMBAs in wound closure and bleeding control. The proposed tissue adhesion mechanisms of iCMBAs are schematically shown in Fig. 9. Upon dropping iCMBA solution inside the full-thickness cutaneous incisions, created on the back of Sprague–Dawley rats,

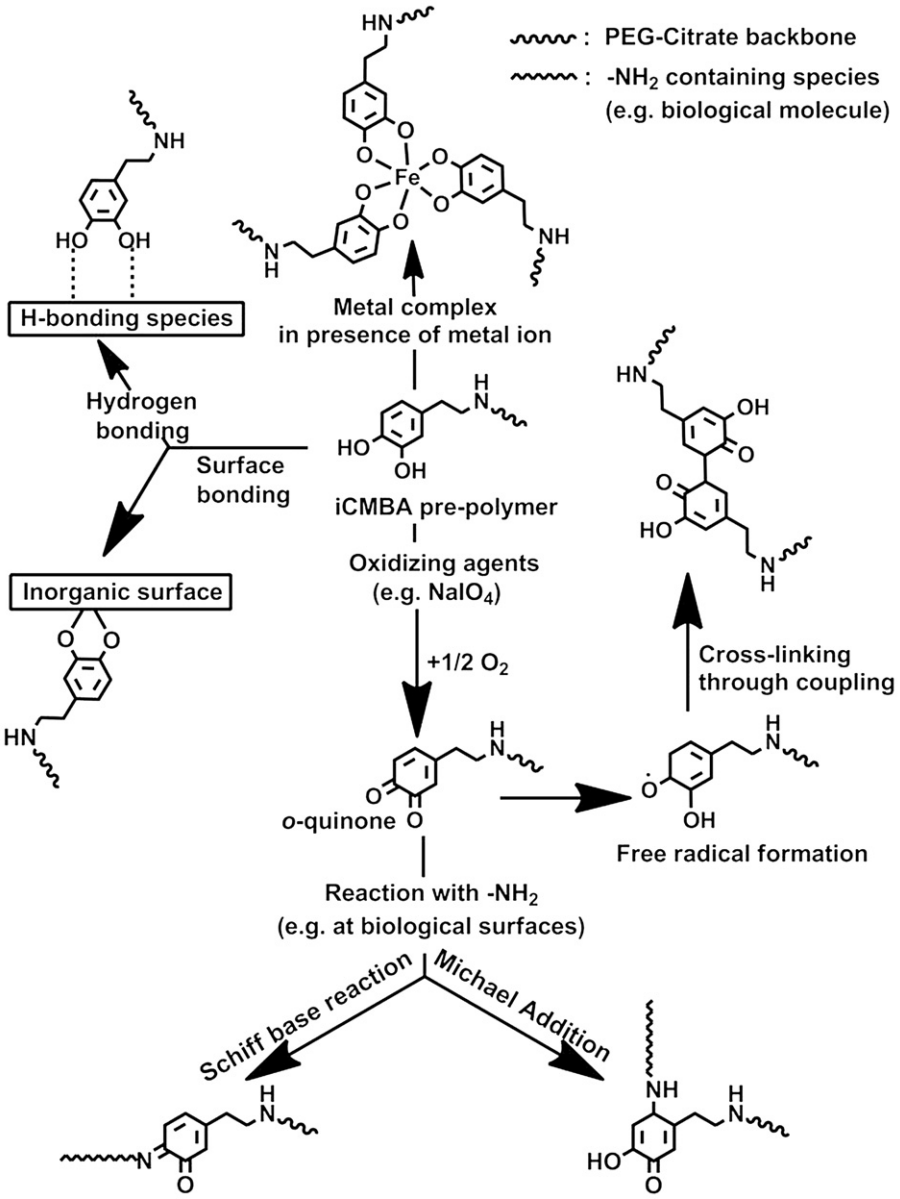

Fig. 8. Schematic representation of possible crosslinking and adhesion pathways of iCMBA pre-polymers.

the bleeding was immediately ceased and the wound opening was closed within a few minutes (Fig. 6A). In contrary to suture, no blood leakage was then sighted, which could be related to superior hemostatic property of iCMBAs to suture. In addition to the formation of a mechanical barrier against blood loss due to the bulk of adhesive, the hemostatic effects of iCMBAs could also partially attributed to the rich carboxyl groups on iCMBAs, which can readily interact with blood protein to form insoluble interpolymeric complexes. In addition, using iCMBA lead to an improved and accelerated wound healing when compared to suture (Figs. 6B, C and 7A–C). The histological evaluation (H&E staining) at 7th day post application of iCMBAs showed only minor acute inflammation, while total cell infiltration into the incision area at both 7th and 28th day time points, defined by cell density, was not significantly different for iCMBA-treated and sutured wounds (Fig. 6D–G, P). Moreover, the insignificant difference between number of CD11b positive inflammatory cells in the proximity of iCMBA-treated and sutured wounds at 7th day post treatment indicated the minimal inflammatory response to iCMBA. After 28 days the number of inflammatory cells for both groups was negligible (Fig. 6H–K, Q). The existence of slightly higher amount of collagen at the sites of iCMBA-treated wounds compared with sutured wounds (Fig. 6L–O, R) suggests that iCMBAs may be used to improve wound healing with better outcome than suture stitches. The measurement of mechanical properties of the healed rat skin revealed that the iCMBA-treated skin had superior tensile strength (1250 ± 315 kPa) over suture-closed skin (810 ± 355 kPa), while modulus and elongation at break were similar for both (Fig. 7D, E). These findings suggested that the healing process and tissue reconstruction were facilitated by iCMBA polymers, which presumably provided a suitable scaffold for cell growth and tissue repair, accelerating the tissue regeneration process. Interestingly, after 28 days no trace of polymer was observed at the location of healed tissues, a sign of complete in-vivo degradation of the iCMBAs (Fig. 7C). These results support that this family of bioadhesive polymers is suitable candidates for biological applications, particularly where the

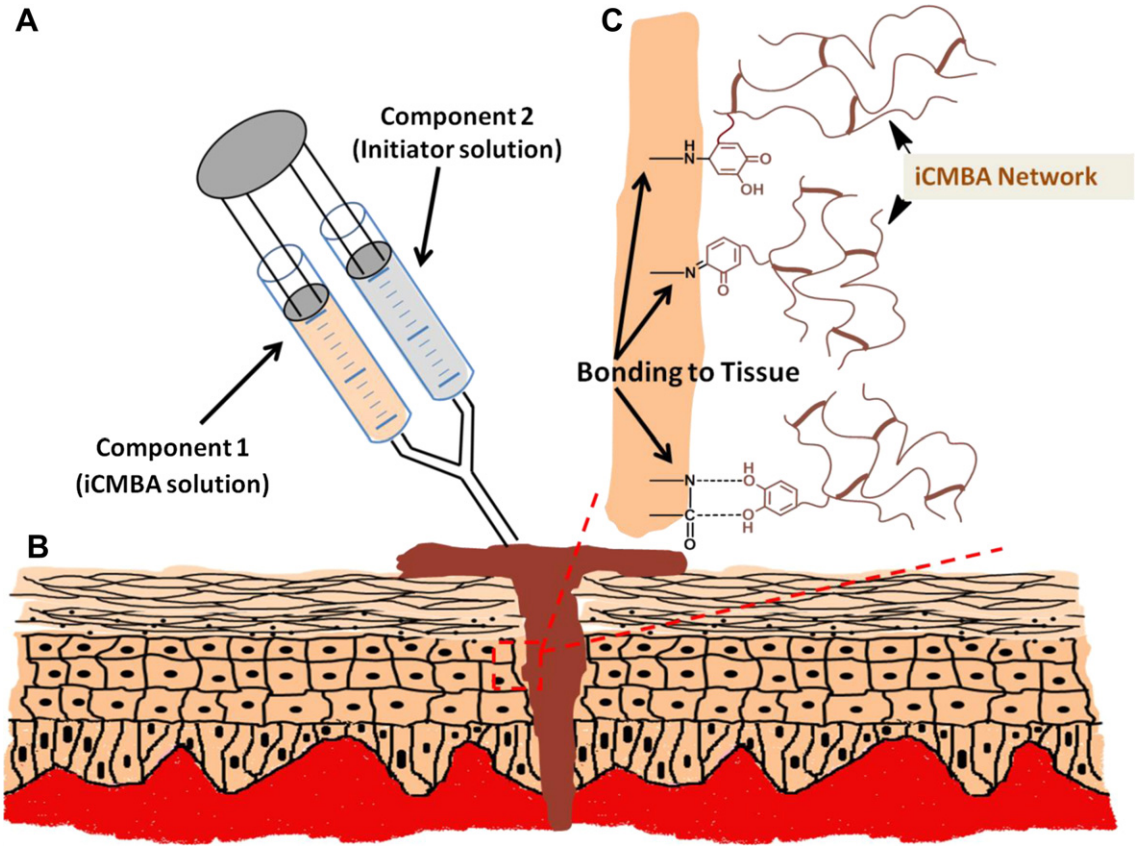

Fig. 9. Schematic of iCMBA application for wound closure. A) Preparation and application of 2-component adhesive: iCMBA and oxidizing (sodium periodate) solutions. B) Schematic representation of iCMBA utilized for sutureless wound closure. C) Proposed mechanisms of iCMBAs adhesion to tissues.

employed biomaterial is required to be degraded and absorbed after intended time of service with minimal toxicity on the host body. Another observed advantage of iCMBA adhesive over suture was the absence of needle holes (wounds), inevitably created in suturing, when using the adhesive, as evident from Fig. 7A–C.

To the best our knowledge, iCMBAs were the first biodegradable strong wet-tissue adhesives that could effectively seal a bleeding open wound (2 cm long × 0.5 cm deep), instantly stop bleeding, and promote tissue regeneration without the aid of other surgical tools, such as suture and staples, or other adhesive mechanisms. The sutureless wound closure may be particularly very useful for those wounds on which sutures are hard to be placed due to the lack of surrounding healthy collagenous structure and fascia supports. The convenient handling procedures, strong tissue adhesion, controlled degradability, and elastomeric mechanical properties make iCMBA promising for any topical and non-topical applications across all disciplines of surgical practice ranging from suture/staple replacement; tissue grafts to treat hernias, ulcers, and burns; hemostatic wound dressing for laparoscopic partial nephrectomy (LPN); waterproof sealants for vascular anastomoses; and treatment of gastrointestinal (GI) fistulas, leaks, mucosal oozing or bleeding, and perforation.

5. Conclusion

The experimental results presented above demonstrate the syntheses of a family of injectable citrate-based mussel-inspired biodegradable adhesives, iCMBAs, from safe and inexpensive constituents and via a one-step synthesis technique without involvement of any toxic reagents, and their applications in hemostasis and sutureless wound closure. The syntheses of iCMBA enrich the methodology of citrate-based biomaterial development and represent an innovation for tissue adhesive biomaterial design.

Acknowledgments

This work was supported in part by R01 awards (EB012575 (to J.Y.) and EB007271 (to L.T.)) from the National Institute of Biomedical Imaging and Bioengineering (NIBIB), and a National Science Foundation (NSF) CAREER award 0954109 (to J.Y.).

References

[1] Spotnitz WD, Burks S. Hemostats, sealants, and adhesives: components of the surgical toolbox. Transfusion 2008;48:1502–16.
[2] Sierra DH. Fibrin sealant adhesive systems: a review of their chemistry, material properties and clinical applications. J Biomater Appl 1993;7:309–52.
[3] Spotnitz WD. Fibrin sealant in the United States: clinical use at the University of Virginia. Thromb Haemost 1995;74:482–5.
[4] Spotnitz WD, Burks SG, Prabhu R. Fibrin-based adhesives and hemostatic agents. In: Quinn JV, editor. Tissue adhesives in clinical medicine. 2nd ed. Hamilton: BC Decker Inc; 2005. p. 77–112.
[5] Radosevich M, Goubran HI, Burnouf T. Fibrin sealant: scientific rationale, production methods, properties, and current clinical use. Vox Sang 1997;72:133–43.
[6] Joch C. The safety of fibrin sealants. Cardiovasc Surg 2003;11(Suppl. 1):23–8.
[7] Traver MA, Assimos DG. New generation tissue sealants and hemostatic agents: innovative urologic applications. Rev Urol 2006;8:104–11.
[8] Albes JM, Krettek C, Hausen B, Rohde R, Haverich A, Borst HG. Biophysical properties of the gelatin-resorcin-formaldehyde/glutaraldehyde adhesive. Ann Thorac Surg 1993;56:910–5.
[9] Conrad K, Yoskovitch A. The use of fibrin glue in the correction of pollybeak deformity: a preliminary report. Arch Facial Plast Surg 2003;5:522–7.
[10] Brennan M. Fibrin glue. Blood Rev 1991;5:240–4.
[11] Quinn JV. Tissue adhesives in clinical medicine. In: Quinn JV, editor. Tissue adhesives in clinical medicine. 2nd ed. Hamilton: BC Decker Inc; 2005. p. 27–76.

[12] Shalaby SW, Shalaby WSW. Cyanoacrylate-based systems as tissue adhesives. In: Shalaby SW, Burg KJL, editors. Absorbable and biodegradable polymers. Boca Raton: CRC Press; 2004. p. 59–75.
[13] Wheat JC, Wolf Jr JS. Advances in bioadhesives, tissue sealants, and hemostatic agents. Urol Clin North Am 2009;36:265–75 [x].
[14] Waite JH. Nature's underwater adhesive specialist. Int J Adhes Adhes 1987;7:9–14.
[15] Waite JH. Adhesion à la Moule. Integr Comp Biol 2002;42:1172–80.
[16] Waite JH, Tanzer ML. The bioadhesive of *Mytilus byssus*: a protein containing L-dopa. Biochem Biophys Res Commun 1980;96:1554–61.
[17] Strausberg RL, Link RP. Protein-based medical adhesives. Trends Biotechnol 1990;8:53–7.
[18] Waite JH, Qin X. Polyphosphoprotein from the adhesive pads of *Mytilus edulis*. Biochemistry 2001;40:2887–93.
[19] Deming TJ. Mussel byssus and biomolecular materials. Curr Opin Chem Biol 1999;3:100–5.
[20] Waite JH. The phylogeny and chemical diversity of quinone-tanned glues and varnishes. Comp Biochem Physiol B 1990;97:19–29.
[21] Lin Q, Gourdon D, Sun C, Holten-Andersen N, Anderson TH, Waite JH, et al. Adhesion mechanisms of the mussel foot proteins mfp-1 and mfp-3. Proc Natl Acad Sci U S A 2007;104:3782–6.
[22] Lee H, Scherer NF, Messersmith PB. Single-molecule mechanics of mussel adhesion. Proc Natl Acad Sci U S A 2006;103:12999–3003.
[23] Yu M, Deming TJ. Synthetic polypeptide mimics of marine adhesives. Macromolecules 1998;31:4739–45.
[24] Tatehata H, Mochizuki A, Kawashima T, Yamashita S, Yamamoto H. Model polypeptide of mussel adhesive protein. I. Synthesis and adhesive studies of sequential polypeptides (X-Tyr-Lys)(n) and (Y-Lys)(n). J Appl Polym Sci 2000;76:929–37.
[25] Lee BP, Dalsin JL, Messersmith PB. Synthesis and gelation of DOPA-modified poly(ethylene glycol) hydrogels. Biomacromolecules 2002;3:1038–47.
[26] Wang J, Liu C, Lu X, Yin M. Co-polypeptides of 3,4-dihydroxyphenylalanine and L-lysine to mimic marine adhesive protein. Biomaterials 2007;28:3456–68.
[27] Westwood G, Horton TN, Wilker JJ. Simplified polymer mimics of cross-linking adhesive proteins. Macromolecules 2007;40:3960–4.
[28] Brubaker CE, Kissler H, Wang LJ, Kaufman DB, Messersmith PB. Biological performance of mussel-inspired adhesive in extrahepatic islet transplantation. Biomaterials 2010;31:420–7.
[29] Lee H, Dellatore SM, Miller WM, Messersmith PB. Mussel-inspired surface chemistry for multifunctional coatings. Science 2007;318:426–30.
[30] Fan XW, Lin LJ, Dalsin JL, Messersmith PB. Biomimetic anchor for surface-initiated polymerization from metal substrates. J Am Chem Soc 2005;127:15843–7.
[31] Mahdavi A, Ferreira L, Sundback C, Nichol JW, Chan EP, Carter DJD, et al. A biodegradable and biocompatible gecko-inspired tissue adhesive. Proc Natl Acad Sci U S A 2008;105:2307–12.
[32] Lee H, Lee BP, Messersmith PB. A reversible wet/dry adhesive inspired by mussels and geckos. Nature 2007;448:338–41.
[33] Yang J, Webb AR, Pickerill SJ, Hageman G, Ameer GA. Synthesis and evaluation of poly(diol citrate) biodegradable elastomers. Biomaterials 2006;27:1889–98.
[34] Yang J, Motlagh D, Allen JB, Webb AR, Kibbe MR, Aalami O, et al. Modulating expanded polytetrafluoroethylene vascular graft host response via citric acid-based biodegradable elastomers. Adv Mater 2006;18:1493–8.
[35] Yang J, Webb AR, Ameer GA. Novel citric acid-based biodegradable elastomers for tissue engineering. Adv Mater 2004;16:511–6.
[36] Qiu HJ, Yang J, Kodali P, Koh J, Ameer GA. A citric acid-based hydroxyapatite composite for orthopedic implants. Biomaterials 2006;27:5845–54.
[37] Dey J, Xu H, Shen JH, Thevenot P, Gondi SR, Nguyen KT, et al. Development of biodegradable crosslinked urethane-doped polyester elastomers. Biomaterials 2008;29:4637–49.
[38] Dey J, Xu H, Nguyen KT, Yang JA. Crosslinked urethane doped polyester biphasic scaffolds: potential for in vivo vascular tissue engineering. J Biomed Mater Res A 2010;95A:361–70.
[39] Gyawali D, Nair P, Zhang Y, Tran RT, Zhang C, Samchukov M, et al. Citric acid-derived in situ crosslinkable biodegradable polymers for cell delivery. Biomaterials 2010;31:9092–105.
[40] Tran RT, Thevenot P, Gyawali D, Chiao JC, Tang LP, Yang J. Synthesis and characterization of a biodegradable elastomer featuring a dual crosslinking mechanism. Soft Matter 2010;6:2449–61.
[41] Yang J, Gyawali D, Stark JM, Akcora P, Nair P, Tran RT, et al. A rheological study of biodegradable injectable PEGMC/HA composite scaffolds. Soft Matter 2012. http://dx.doi.org/10.1039/c1sm05786c.
[42] Yang J, Zhang Y, Gautam S, Liu L, Dey J, Chen W, et al. Development of aliphatic biodegradable photoluminescent polymers. Proc Natl Acad Sci U S A 2009;106:10086–91.
[43] Yang J, Zhang Y, Gautam S, Liu L, Dey J, Chen W, et al. Development of aliphatic biodegradable photoluminescent polymers [vol. 106, pg 10086, 2009]. Proc Natl Acad Sci U S A 2009;106:11818–9.
[44] Graham DG, Jeffs PW. The role of 2,4,5-trihydroxyphenylalanine in melanin biosynthesis. J Biol Chem 1977;252:5729–34.
[45] Jorgensen PH, Jensen KH, Andreassen TT. Mechanical strength in rat skin incisional wounds treated with fibrin sealant. J Surg Res 1987;42:237–41.
[46] Abramoff MD, Magelhaes PJ, Ram SJ. Image processing with ImageJ. Biophotonics Int 2004;11:36–42.
[47] Xie D, Chen D, Jiang B, Yang C. Synthesis of novel compatibilizers and their application in PP/nylon-66 blends. I. Synthesis and characterization. Polymer 2000;41:3599–607.
[48] Deming TJ, Yu ME, Hwang JY. Role of L-3,4-dihydroxyphenylalanine in mussel adhesive proteins. J Am Chem Soc 1999;121:5825–6.
[49] Barroso-Bujans F, Martinez R, Ortiz P. Structural characterization of oligomers from the polycondensation of citric acid with ethylene glycol and long-chain aliphatic alcohols. J Appl Polym Sci 2003;88:302–6.